Proceedings of the 4th WSEAS International Conference on Fluid Mechanics and Aerodynamics, Elounda, Greece, August 21-23, 2006 (pp68-74)

Interaction between Boundary Layer and Shock in Hypersonic Flows with chemical real gas effects

Nabi Jahantigh[1], M.Mirzaei[2], A. Shadaram[3]
Mechanical engineering department
Zabol University
Jahad square - Zabol
Iran

ABSTRACT

In this paper, viscous interaction phenomenon in hypersonic flows with chemical reactions is numerically simulated. Two-dimensional Navier-Stokes equations are solved to simulate this phenomenon. Inviscid fluxes are approximated using Van Leer flux vector splitting method and to increase the accuracy of this approximation, MUSCL approach with Van albada limiters is applied. Chemical reactions are considered to be in equilibrium conditions. With this assumption there is no closed form for equation of state for the gas (air) and relation between thermodynamic properties are calculated from thermodynamic tables. In addition, transport properties (viscosity and conductivity) are functions of two independent thermodynamic properties. These functions are calculated using kinetic theory. To evaluate the performance of the model used in this research, some test cases are studied. First test case is flow over a ramp with various angles. The results of this test case are compared with the results of other numerical methods and the effect of geometry on separation length is studied. The second case is a hypersonic flow over a 15-degree ramp. The results are in good agreement compared with experimental data. In addition, there results are compared with the results of ideal gas (non-reacting flow) calculations. It can be seen that ideal gas assumption for air introduces considerable deviation form experimental data.

Keywords: Compressible navier stokes equations- Interaction-Flux vector descretise- Shock waves- Limiter-Chemical reaction

[1] Head of department of mechanics

[2] Assistant Professor

[3] Assistant Professor

1 Introduction

Viscous interaction is one of the major aspects of hypersonic flows. Interaction between a shock wave and a boundary layer can produce a region of separated flow. The phenomenon may occur, for example, at the upstream-facing corner formed by deflected control surface on a hypersonic reentry vehicle, where the length of separation has implications for control effectiveness. Separation can also occur where a shock wave generated internally to a hypersonic air-breathing propulsion system impinges on a boundary layer. Thus separation length may be important in determining engine performance. In addition, knowledge regarding separation length in shock/boundary-layer interactions has relevance to separation length in supersonic wake flow. Various experimental and numerical works have been carried out to simulate this problem. Since this problem involves downstream effects, especially in separation regions, models based on boundary layer theory or parboiled Navier-stokes (PNS) lead to inaccurate results. So, usually full Navier-Stokes equations are employed to analyze this problem [1-5]. This phenomenon is normally simultaneous with fluid chemical reaction due to high temperature effects Because of this; several researchers have considered the effects of chemical reactions [6-11]. These effects are normally called "real gas effects". Chemical reactions, depending on the flow time scale, may be assumed to be in equilibrium [6-8] or in non-equilibrium [9-11] conditions. In this Paper, this problem is modeled using full Navier-Stokes equations and the effects of chemical reaction with equilibrium assumption on the results are evaluated. Separation length, pressure distribution, friction factor, and heat transfer coefficient are parameters, which are studied in this research.

2 Governing Equations

Navier-stokes equations are used to simulate this phenomenon. These equations in conservative form in a generalized coordinate system (ξ,η) are express as follow:

$$\frac{\partial Q}{\partial t}+\frac{\partial E^{i}}{\partial x}+\frac{\partial F^{i}}{\partial y}=\frac{\partial E^{v}}{\partial x}+\frac{\partial F^{v}}{\partial y} \qquad (1)$$

Where, Q is vector of dependent variables, E^i and F^i are in viscid fluxes, and E^v and F^v are Viscous flux. To close the system of equations, relations between thermodynamic variables are required, along with expressions for the transport properties $\overline{\mu}$ and $\overline{k}$. For flow with no chemical reaction, prefect gas equation of state can be used. For transport properties, viscosity is calculated using Sutherland equation and Prandle number is assumed to be constant. For a chemical reacting flow, these correlations are not very simple. In this paper, chemical reactions are considered to be in equilibrium conditions and the working fluid is air. For equilibrium air computations, approximate curve fits are employed to correlate thermodynamic properties and calculation of transport properties. The thermodynamic properties are obtained using the correlations:

$$\begin{aligned} &\tilde{p}=\tilde{p}(\tilde{e},\tilde{\rho}), \quad \tilde{\gamma}=\tilde{\gamma}(\tilde{e},\tilde{\rho}), \quad \tilde{\mu}=\tilde{\mu}(\tilde{e},\tilde{\rho}) \\ &\tilde{h}=\tilde{h}(\tilde{p},\tilde{\rho}), \quad \tilde{T}=\tilde{T}(\tilde{p},\tilde{\rho}), \quad \tilde{T}=\tilde{T}(\tilde{e},\tilde{\rho}) \end{aligned} \qquad (2)$$

Developed by Srinivasan et al.[12], This curve fits Are valid for temperatures up to 15000° K and Density ratio from 10- 7 to 103 . The pressure is Computed using the expression:

$$\tilde{p}=(\tilde{\gamma}-1)\tilde{\rho}\tilde{e} \qquad (3)$$

Here $\tilde{\gamma}$ is defined by:

$$\tilde{\gamma}=\tilde{h}/\tilde{e} \qquad (4)$$

For perfect-gas computation, $\tilde{\gamma}=\gamma_{\infty}$.The curved Fits for the transport properties were also developed by Srinivasan et al. [13], and include the following correlations:

$$\tilde{\mu} = \tilde{\mu}(\tilde{e}, \tilde{\rho}), \qquad \tilde{k} = \tilde{k}(\tilde{e}, \tilde{\rho}) \tag{5}$$

The curves fits are constructed based on kinetic theory and are valid for temperature up to 15000° K and density ratio from 10^{-5} to 10.

3 Numerical Method

Finite volume technique is used to descritize the governing equations in a structural grid and for temporal approximation, simple explicit method is applied. The descritized form of the governing equations in a computational cell is:

$$\Delta Q = -\frac{\Delta t}{\Delta V}\sum_{i=1}^{4}[(F_i - F_v).n\Delta A]_i \tag{6}$$

The next step is approximation of viscous and in viscid fluxes. Viscous fluxes are approximated by central differencing. This approximation is compatible with physical nature of these fluxes. There are various kinds of method to approximate in viscid fluxes on cell boundaries. In this paper Van Leer flux vector splitting is used for this approximation. In this approach, flux vectors are splitted to positive and negative based on local Mach number. Negative fluxes are calculated from left side of a cell boundary and positive fluxes are calculated from right side of the boundary. This method in comparison with other methods such as Stegar-Warming method [14], has better ability in shock capturing. General forms of splitted fluxes are as follow [15]:

$$F^{\pm(n)} = F_{mass}^{\pm(n)} \times \begin{bmatrix} 1 \\ u + \dfrac{n_y(-v_n \pm 2c)}{\gamma} \\ v + \dfrac{n_y(-v_n \pm 2c)}{\gamma} \\ \dfrac{\vec{V}^2 - v_n^2}{2} + \dfrac{[(\gamma-1)v_n \pm 2c]^2}{2(\gamma^2-1)} \end{bmatrix} \tag{7}$$

$$F_{mass}^{\pm(n)} = \pm\frac{\rho c(M_n \pm 1)^2}{4} \tag{8}$$

Where u and v are velocity components in Cartesian coordinate system, c is local sonic velocity, M_n is local Mach number based on normal velocity, n_x ,n_y are components of unit vector normal to cell boundary v_n is velocity component in normal direction. The lateral flux for function Φ has the following form:

$$(\rho v) = F^{+}_{mass,B}\phi_B + F^{-}_{mass,T}\phi_T \tag{9}$$

Or

$$(\rho v) = \left(F^{+}_{mass,B} + F^{-}_{mass,T}\right)\left(\frac{\phi_B + \phi_T}{2}\right) - \left(F^{+}_{mass,B} - F^{-}_{mass,T}\right)\left(\frac{\phi_T - \phi_B}{2}\right) \tag{10}$$

The first term of equation (9) indicates a central approximation and the second terms shows numerical diffusion. If one of the fluxes is plotted versus Mach number, it can be seen that for zero Mach number, splitted flux is not zero. So if we define such a function that results zero splitted flux at zero Mach number, numerical diffusion will be zero. Since first order Van Leer scheme presents numerical diffusion error, MUSCL approximation [16] is used to remove this drawback, In this approximation, $Q^{L}_{i+1/2,j}$, $Q^{R}_{i+1/2,j}$ are defined as follow:

$$Q^{L}_{i+1/2,j} = Q_{i,j} + .0.25[\overline{\Psi}^{L}(1 - K\overline{\Psi}^{L}) \times (Q_{i,j} - Q_{i-1,j}) + \overline{\Psi}^{L}(1 + K\overline{\Psi}^{L}) \times (Q_{i+1,j} - Q_{i,j})] \tag{11}$$

And

$$Q^{R}_{i+1/2,j} = Q_{i,j} - .0.25[\overline{\Psi}^{R}(1 - K\overline{\Psi}^{R}) \times (Q_{i+2,j} - Q_{i+1,j}) + \overline{\Psi}^{R}(1 + K\overline{\Psi}^{R}) \times (Q_{i+1,j} - Q_{i,j})] \tag{12}$$

Where $\overline{\Psi}^{L}$ and $\overline{\Psi}^{R}$ are limiters which are used to suppress numerical oscillations. In this paper Val Albada limiters [16] is applied. The general forms of these limiters are as follow:

$$\overline{\Psi}^{R} = \frac{2[(Q_{i+2,j} - Q_{i+1,j}) \times (Q_{i+1,j} - Q_{i,j})] + \varepsilon}{(Q_{i+2,j} - Q_{i+1,j})^2 + (Q_{i+1,j} - Q_{i,j})^2 + \varepsilon} \tag{13-a}$$

$$\overline{\Psi}^{L} = \frac{2[(Q_{i+1,j} - Q_{i+1,j}) \times (Q_{i,j} - Q_{i-1,j})] + \varepsilon}{(Q_{i+1,j} - Q_{i+1,j})^2 + (Q_{i,j} - Q_{i-1,j})^2 + \varepsilon} \qquad (13\text{-b})$$

Where, 1c is the cell size, $\overline{V}$ flow velocity, and c local sonic velocity

4 Results

Two test cases have been carried out and the results are compared with the results of other numerical methods and experimental data.

4.1 Case1:

The first problem is flow over a compression corner with the following free stream condition:

$M_\infty = 3.$, $T_\infty = 216^\circ K$, $Re_L = 1.68 \times 10^4$

The ramp is in constant temperature of 660 K in this problem downstream effects are very strong. Figures 1 to 4 show the results of this problem. The results are obtained from the solution of the problem in grid with 52 non-uniform distributed points in lateral direction and 101 uniform distributed in longitudinal direction This grid size insures us for grid independency of the results. Figure 1 shows pressure coefficient along the ramp for ramp angle of 10 degree. In this figure, the results of present calculations are compared with the results of Navier-Sokes calculation reference [1]. Good agreement can be seen between these two results. Stanton number distribution along 10 degree ramp is shown in figure 2. In this figure, the results of this study are compared with other Navier-Stokes calculation presented in reference [1] and [2]. We can see that Stanton number distribution predicted by the present scheme has excellent agreement with the results of [1] and [2]. One of the major parameter in viscous interaction problem is separation length. This parameter is a function of flow conditions and geometry. For this case the effect of geometry on the separation length is shown in figure 3. It can be seen that increasing the ramp angle causes increasing the separation length. Figure 4 shows streamlines around the separation region for a 25-degree ramp.

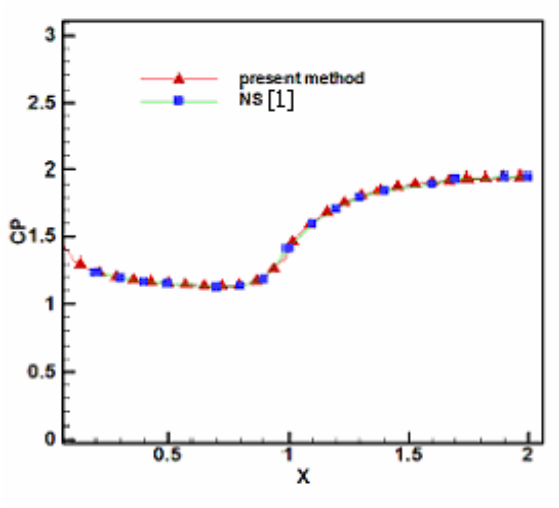

Fig.1: Pressure coefficient along 10 degree ramp

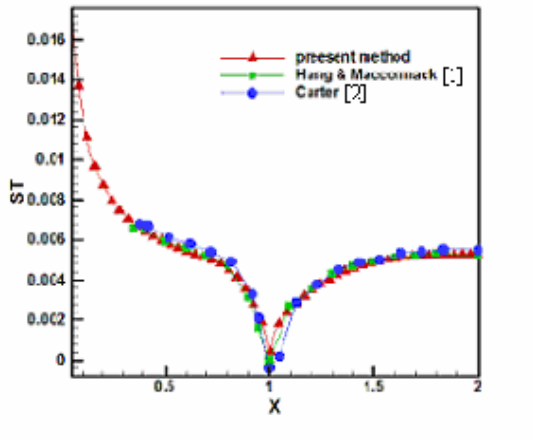

Figure 2 Stanton Number for case 1

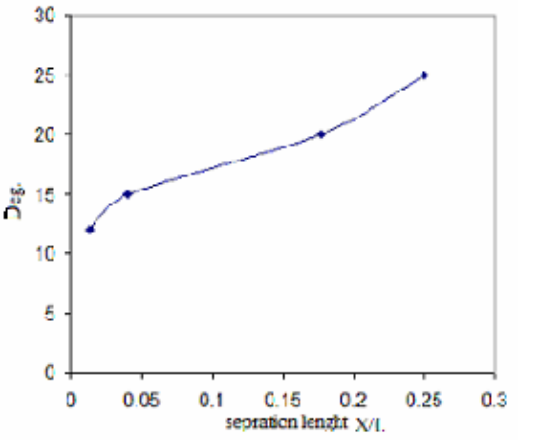

Figure 3: Effect of ramp angle on separation length

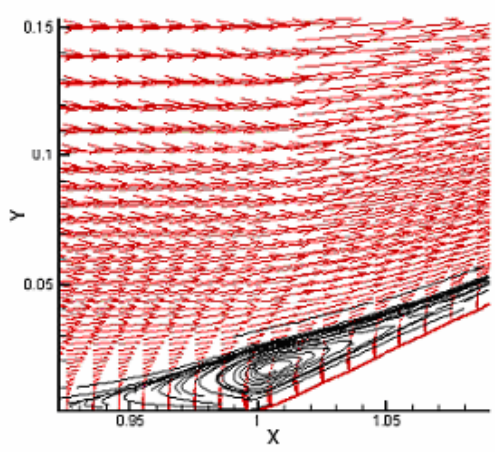

Fig.4 : Streamline around region separation

4.2 Case 2:

In this case, we study hypersonic flow over a 15-degree ramp with the following free stream conditions:

$M_\infty = 7.5$, $Re_L = 4.08 \times 10^5$, $T_\infty = 940^\circ K$

$u_\infty = 4.20 km/s$, $\rho_\infty = 3.43 \times 10^{-3} kg/m^3$

For this test case, experimental data are available and the results of the present study are compared with this experimental data. The results of the above-mentioned case are presented in figures.3 to 6. Figure 5 shows pressure coefficient distribution along the body. In this figure, the results of the present research are compared with ideal gas calculations (with on chemical reaction assumption) and experimental data [8]. It can be seen That no chemical reaction assumption (which is normally refered to as ideal gas assumption) for air introduces considerable deviation form experiment. Conversely, the chemical reaction assumption leads to good agreement of the numerical calculation with the experimental data. In addition, figure 6 shows the variation of Stanton number along the body. In this figure, the results of real gas (chemical reaction) calculation are compared with the results of no reacting flow calculation and experiment [8]. This comparison shows that the inclusion of chemical reaction for gas is an important factor for simulation of such flow fields. Pressure profiles for this problem are plotted in figure 7. In this figure pressure profile of real gas calculations is compared with that of ideal gas calculation at section of x/l=1.8. This figure shows a considerable difference between these two results. In addition, in figure 8, temperature profiles of both real gas and ideal gas calculations at x/l=1.8 is presented. The trend is similar to pressure profiles; the difference between these two temperature profiles calculations is considerable. Figure 9 shows temperature contours for real gas and ideal gas calculations. Thickness of Shock layer in the flow field with chemical reaction is less than that in the flow field with no chemical reaction assumption. This is due to density effect. Actually, temperature predicted by real gas assumption is less than that of ideal gas. Therefore, calculated density from real gas will be less than that of ideal gas and higher density causes smaller shock layer thickness.

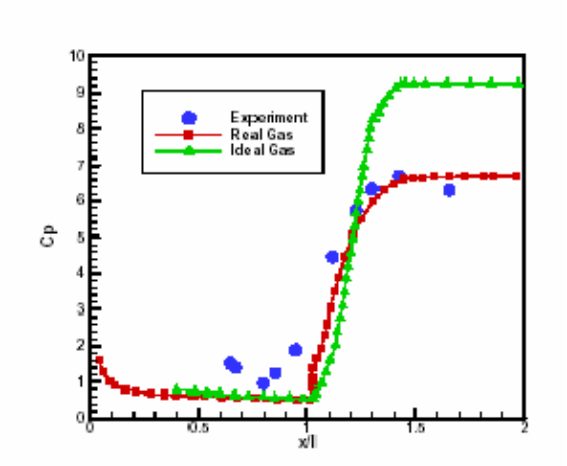

Fig.5: Pressure coefficient Distribution

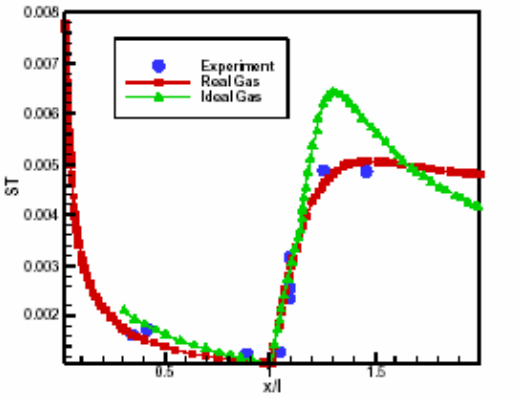

Fig.6: Stanton number Distribution

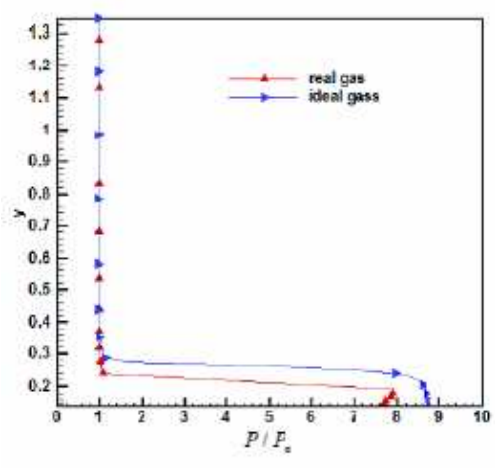

Fig. 7: Pressure Profiles at x/l=1.8

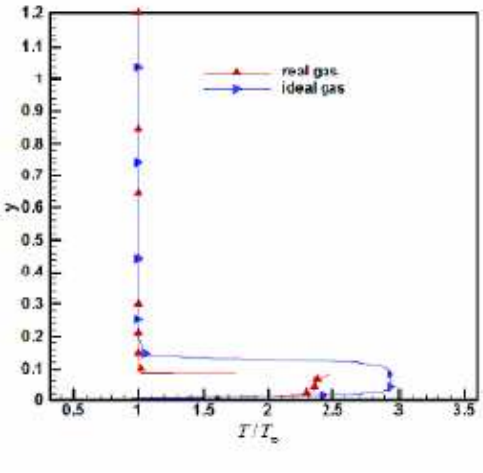

Fig. 8: Temperature Profile at x/l=1.8

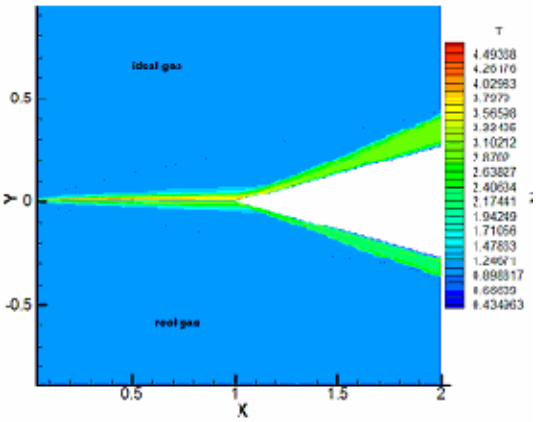

Fig 9: Temperature contours

5 Conclusion

In this paper viscous interaction phenomenon was analyzed numerically and the effects of chemical reaction on flow parameters such as separation length, pressure coefficient and were investigated. The calculated results show that with out inclusion the chemical reaction in flow calculation may leads to consider able deviation from experimental data

6 Referances

[1] Hung, C. M. And McCormack, R.W. "Numerical solution for supersonic and hypersonic laminar compression corner" NASA, TR-385 July, 1972.

[2] Carter, J.E., "Numerical solutions of the Na vier- Stokes equations for supersonic flow over a two Dimensional compression corner" NASA TR R-385, July 1972

[3] Bloy , A. W. And Georgeff, M. P., "The hypersonic laminar boundary layer near sharp compression and expansion corners", Journal of Fluid Mechanics 63, 431 (1974).

[4] Holden, M. "A study of flow separation in regions of shock wave-boundary layer interaction in hypersonic flow", AIAA Paper 78-1169 (1978).

[5] Fay, J. F. Sambamurthi, , J. ,"Laminar hypersonic flow over a compression corner using the HANA code", AIAA Paper 92-289 6 (1992).

[6] Grasso, F., Leone, G. "Chemistry effects in shock wave boundary layer interaction problems", in Proceedings of the IUTAM Symposium on Aerothermochemsitry of Spacecraft and Associated Hypersonic Flows (Jouve, Paris, 1992).

[7] Mcintosh, M. K. "Computer program for the numerical calculation of equilibrium and perfect gas conditions in shock tunnels"

Proceedings of the 4th WSEAS International Conference on Fluid Mechanics and Aerodynamics, Elounda, Greece, August 21-23, 2006 (pp68-74)